Journal of the European Ceramic Society 20 (2000) 1091–1098

Melt extraction processing of structural Y_2O_3–Al_2O_3 fibers

E.A. Aguilar*, R.A.L. Drew

Department of Mining and Metallurgical Engineering, McGill University, 3610 University, Montreal, Quebec, Canada H3A 2B2

Received 5 August 1999; accepted 5 October 1999

Abstract

Compounds in the system Y_2O_3-Al_2O_3 are promising materials for optical, electronic and structural applications. In this study, a melt extraction process with a new approach to making ceramic fibers was used to produce amorphous fibers in the Y_2O_3–Al_2O_3 system within the 20–30-micron size range. Smooth and uniform cross section fibers with relatively high tensile strength were obtained depending on the wheel velocity. X-ray diffraction of as-extracted fibers revealed the non-crystalline nature of the yttria-alumina compositions. The crystallization and glass transition temperatures of non-crystalline fibers were determined using differential thermal analysis (DTA). Crystalline phases were identified by X-ray diffraction in the fibers after heat treatment.

Keywords: Fibres; Mechanical properties; Melt extraction; Structural applications; Y_2O_3–Al_2O_3

1. Introduction

Continuous oxide ceramic fibers are attractive as reinforcing phases for high-temperature structural materials since they combine high strength and elastic modulus with high-temperature capabilities and a general freedom from environmental attack. They also possess good thermal properties because of their higher melting points and lower thermal expansion coefficients. The incorporation of ceramic fibers into polymers, metal alloys, and ceramics produces composite materials with superior properties.[1,2]

Motivated by aerospace applications requiring composite materials that are lightweight, stiff, and strong, fiber research and development efforts over the last two decades have resulted in a variety of commercially available high performance, continuous fibers with low densities (<4 gm/cm^3), high Young's moduli (>200 GPa), and high tensile strengths (>1 GPa). However, for certain applications requiring high structural reliability, very few of these fibers are ideally suited as reinforcement for either metal matrix composites (MMC) or ceramic matrix composites (CMC). That is, in their current production state, these commercial fibers fail to meet all the necessary property requirements for providing MMC or CMC with high strength and toughness.[3,4]

Applications are emerging for structural materials that involve cyclic-stress, cyclic-temperature duty cycles at temperatures in excess of 1350°C in oxidizing conditions. The use of oxide fibers as strengthening and toughening elements in high temperature metal-, intermetallic- and ceramic-matrix composites represents one of the few approaches for making parts which can satisfy these difficult requirements. Oxide fiber reinforcements do not suffer from oxidation, and also many oxides combine the high melting points and low densities that are crucial for high temperature aerospace applications.[5]

On the other hand, the system Y_2O_3–Al_2O_3 is a promising material for refractory coatings and for ceramic and semiconductor technologies. Doped single crystals of yttrium aluminates are widely used in lasers and polycrystalline yttrium aluminium oxide ceramics are a very important family of advanced ceramic materials. In addition, the translucent ceramics of this system are known to be useful optical materials. The compound $3Y_2O_3{\cdot}5Al_2O_3$, referred to as yttrium aluminum garnet or YAG, has been used widely as a laser host material.[6] It has promising properties for applications such as high temperature coatings and high temperature structural components. For structural applications, the bulk material may be used in the monolithic form or as the matrix phase for composites. In either case, an important requirement is that the fabricated material must have nearly full density and a controlled grain size.

* Corresponding author.

0955-2219/00/$ - see front matter
PII: S0955-2219(99)00279-4

Although their potential as a matrix material has been investigated,[7–12] there is a relatively little known about the behavior of YAG and Al_2O_3–YAG eutectic fibers, as those which exist are still in the developmental stages. Al_2O_3–YAG eutectic fibers have been produced using an edge-defined film-fed growth technique (EFG) and a laser heated float zone method (LHFZ)[13–15] and exhibit properties substantially better than those reported for monolithic ceramics prepared in a similar manner. Morscher[16] has investigated the creep behavior of YAG fibers prepared using alkoxide sol–gel precursor. King[17,18] has prepared YAG fibers by dry spinning solutions of yttrium and aluminum carboxylate polymers (precursor route) and by dry spinning aqueous oxide sols (sol–gel route). Other investigations have produced Al_2O_3–YAG eutectic and YAG fibers by using the sol–gel method,[19,20] using alkoxides, aqueous and metal oxohydroxopropionates precursors and by extrusion of a mixture of a thermoplastic polymer and YAG powder.[21] Recently, YAG glass fibers were produced by pulling from undercooled molten oxide precursor.[22]

This paper will demonstrate the potential production of a range of amorphous fiber compositions in the Y_2O_3–Al_2O_3 system using the melt extraction technique.

2. Experimental procedure

2.1. Melt extraction

Fabrication of fine oxide ceramic fibers using the melt extraction system is a novel technique developed at McGill University.[23–26] This system is a combination of the crucible melt extraction and pendant drop melt extraction processes that makes it feasible to melt and extract a small volume of high melting, inviscid oxide ceramic in a controlled and reproducible fashion.

The schematic of the melt extraction system is shown in Fig. 1. The extraction wheel is a 14.5-cm-diameter sharpened copper–beryllium-alloy disk (alloy C17 500). Copper was chosen because of its good thermal conductivity necessary to extract the heat from the liquid and to promote rapid solidification. The oxy-acetylene torch is used as a heat source and boron nitride is used only as a guide for the ceramic rods since the molten drop is self-contained by surface tension.

Prior to the extraction, a ceramic rod is melted with the oxyacetylene flame to form a small drop just beneath the wheel tip. Using oxy-acetylene heating, the temperature of the molten drop is ~2000°C. The droplet is then slowly pushed towards the rotating wheel to provide a fine contact between the wheel tip and molten drop. Upon contact with the wheel, the fibers form and rapidly solidify.

2.2. Starting materials

In order to carry out the experiments, aluminum oxide (A17, Alcoa Industrial Chemical Division) with 99.7% purity and yttrium oxide (Grade 5600, Union Molycorp) with 99.99% purity were used. The stoichiometric amounts for Y:Al = 3:5 and eutectic compositions Al_2O_3–YAG eutectic (E1) and YAG–YAP eutectic (E2) were mixed and attrition milled for 2 h using alumina balls and water as media and fluid, respectively (Fig. 2 and Table 1). The resultant slurry was dried for 20 min in a microwave oven.

The 3-mm-diameter ceramic rods were made by extrusion of the ceramic powder using water, and 8% of hydroxypropyl cellulose as a plasticizer, and dried for 24 h in air. They then were fired at 1500°C for 1 h prior to their use for melt extraction.

2.3. Fiber evaluation methods

In order to determine the phases present in the samples and the degree of crystallinity, X-ray diffraction was performed on the samples. A Phillips diffractometer with Cu K_α radiation was used in a range of angles of 2θ from 10° to 80°. To determine the crystallization and glass transition temperatures of the amorphous fibers and the change in phase assemblage, DTA (Perkin–Elmer DTA 7) was performed, heating to 1400°C at a rate of 20°C/min. The resulting samples were X-rayed to detect and identify phases formed upon devitrification. Scanning electron microscopy (SEM) was used to evaluate the surface morphology, the fiber diameter, and the fracture surface.

Tensile strength of glass fibers was measured using an Instron material testing machine operated under computer

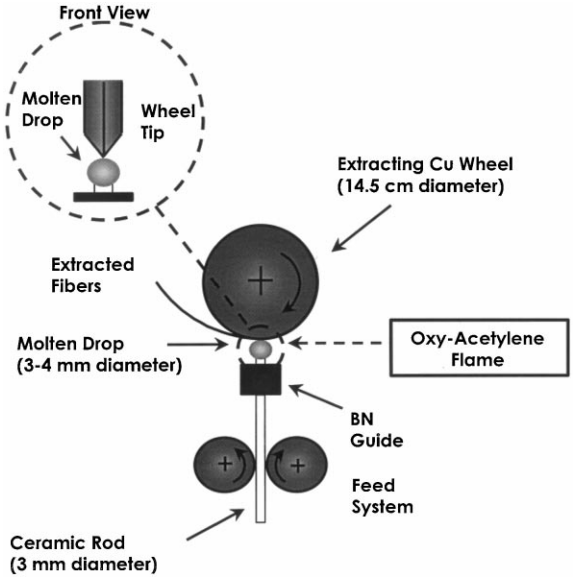

Fig. 1. Schematic diagram of the melt extraction system.

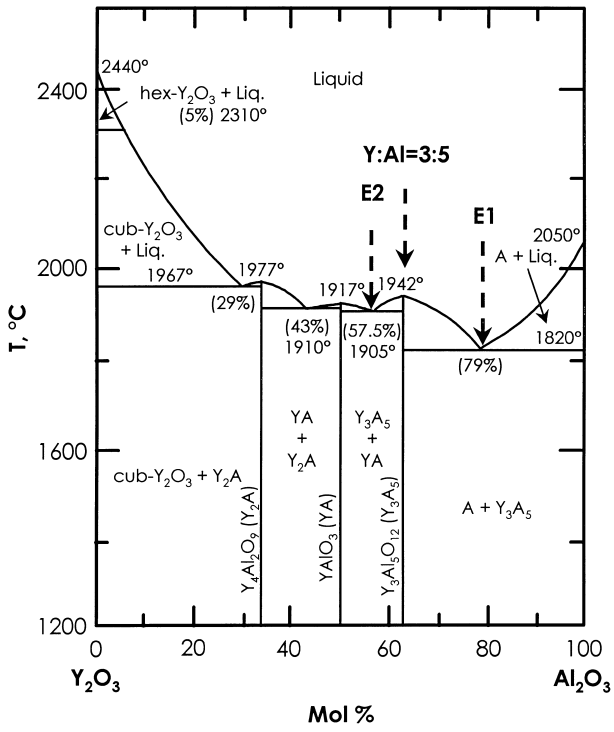

Fig. 2. Y_2O_3–Al_2O_3 phase diagram.[27]

Table 1
Chemical compositions and approximate melting temperatures of the mixtures studied

Composition	Al_2O_3 [wt% (mol%)]	Y_2O_3 [wt% (mol%)]	Melting point (°C)
E1	62.9 (79.0)	37.1 (21.0)	1820
Y:Al = 3:5	43.0 (62.5)	57.0 (37.5)	1942
E2	37.9 (57.5)	62.1 (42.5)	1905

control. The fiber diameters were 20–30 μm, the gauge length was fixed at 30 mm, approximately 1000 times that of the fiber diameter. Test fibers were bonded into a specially designed paper frame with epoxy adhesive. The measurement technique and interpretation was consistent with ASTM standard D3379-75. Fibers were pulled at a constant rate of 2 mm/min. A high sensitivity load cell was used to measure the load. A computer was used to record the load and displacement as a function of time. Broken fibers were examined by optical microscopy to determine the cross section so that stress could be determined.

3. Results and discussion

3.1. Morphology and surface characteristics of extracted fibers

The selected yttria–alumina compositions could be melt extracted and Fig. 3 shows SEM micrographs of

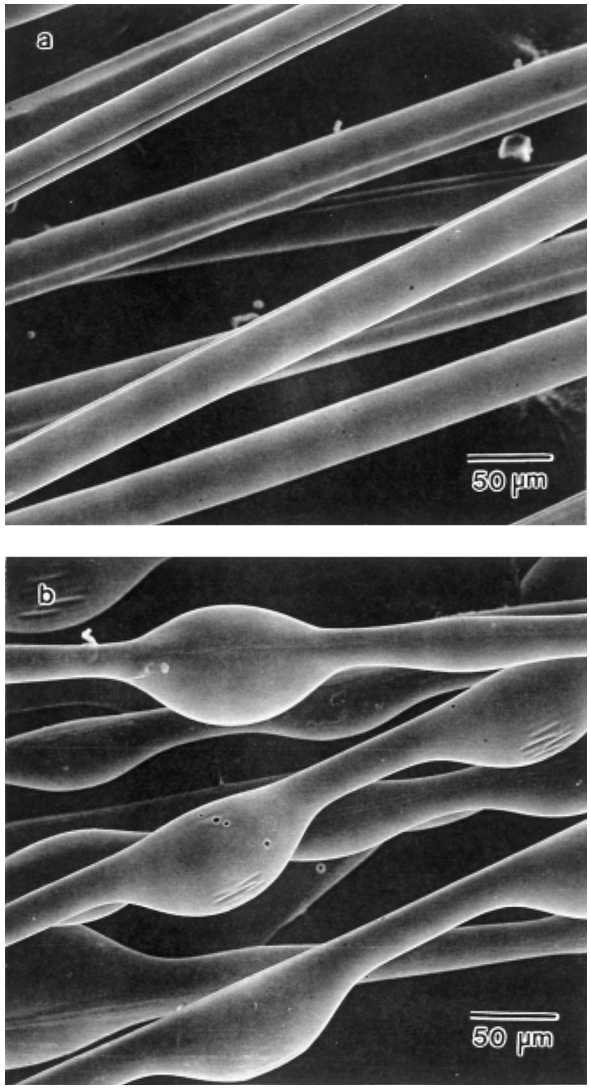

Fig. 3. SEM micrographs of the melt extracted Al_2O_3–YAG eutectic fibers: (a) uniform fibers (1.5 m/s) and (b) fibers exhibiting Rayleigh waves (3.5 m/s).

fibers extracted at different wheel velocities. Generally two types of fibers were obtained: uniform diameter fibers at wheel speeds <3 m/s and fibers exhibiting waves at higher velocities. The fibers produced at speeds <3 m/s had almost circular cross-sections, except at the point of contact with the wheel, and were uniform in diameter. Cross-sectional areas for glass fibers are shown in Fig. 4. For this range, the extracted layer was thin enough to be rapidly solidified by the wheel tip. Under these conditions, no instability occurred within the liquid layer, and uniform diameter fibers were produced with typical diameters of 20–30 μm (Fig. 5a). However, at higher wheel velocities, waves formed on the fibers and the size uniformity decreased. The remaining liquid layer tends to form instabilities which spherodize because of the effects of surface tension attempting to minimize the surface area. Hence the shape of the extracted fiber is no longer uniform. These

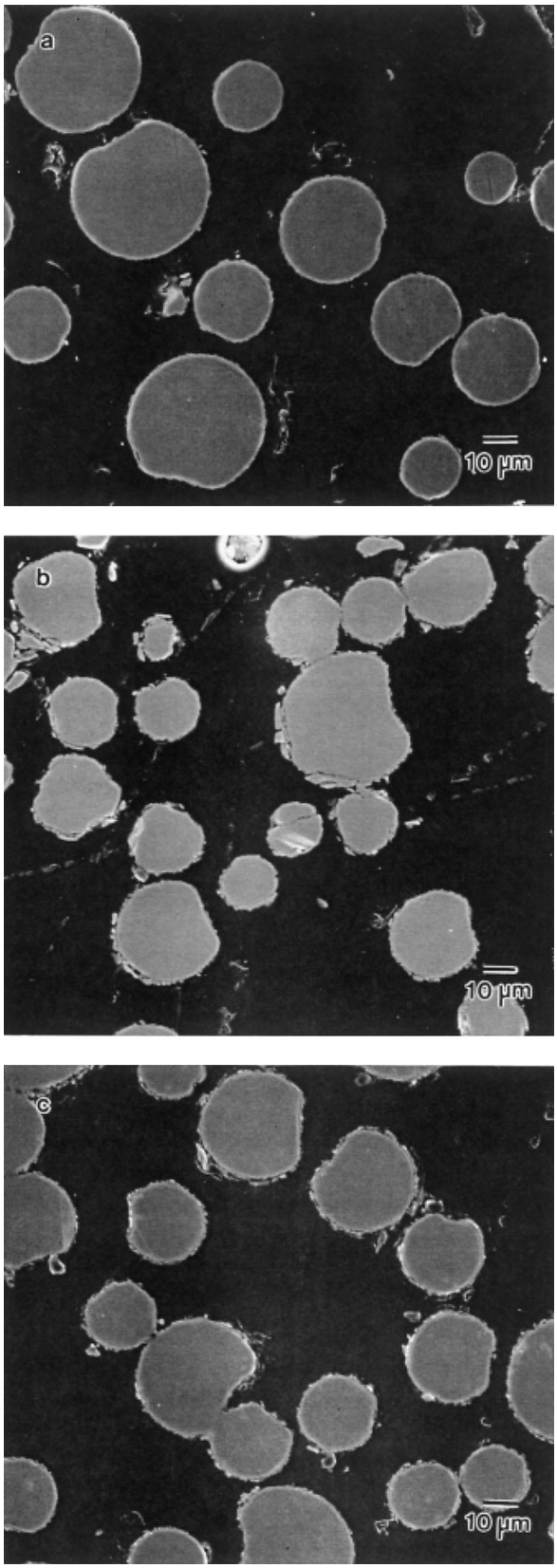

Fig. 4. Cross-sectional areas of as-extracted Y_2O_3–Al_2O_3 fibers: (a) E1, (b) Y:Al = 3:5, and (c) E2.

fibers usually consist of a smooth thin section usually of 20–30 μm diameter with periodic waves of diameters up to 60–70 μm (Fig. 5b).

At higher velocity, more material is extracted, since the rapid extraction pulls a thicker stream of liquid ceramic from the molten drop, which cannot solidify rapidly (the wheel cannot remove heat fast enough). Therefore, the effects of surface tension come into play and waves are formed. The formation of waves has been reviewed in a previous work.[28] This can be divided into three regions as follows: (1) the contact of the wheel tip with the molten drop; (2) the travel length or residence time on the wheel after exit from the molten drop; and (3) the region after separation from the wheel.

During the contact of the wheel tip with the molten drop (region 1), a very thin solid layer starts to form in the contact area, whereas the layer in which the liquid is in motion (i.e. the momentum layer) is much thicker. The extracted layer becomes rapidly thinner as it exits the drop, and reaches a thickness defined as the mean fiber diameter (i.e. the fiber dimension prior to the formation of waves). This layer is extremely thin (of the order of the fiber dimension) and is a mixture of liquid and solid as it travels further on the wheel. During this stage (region 2), the solidification front proceeds towards the free surface of the liquid fiber by conduction into the wheel tip. Meanwhile, the surface tension, which tends to reduce the surface area of the liquid layer, comes into effect, and waves form quickly on the free surface of the fiber.

Solidification shrinkage and cooling of the fiber build up large stresses along the contact area with the wheel

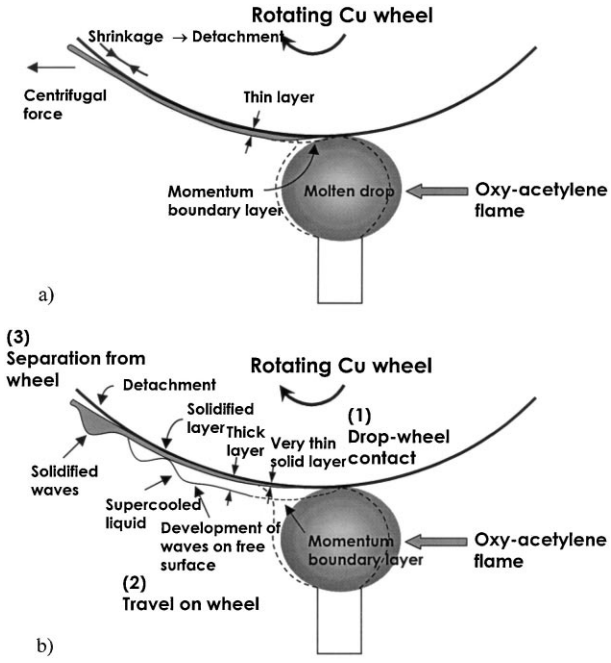

Fig. 5. Schematic diagram of the evolution of (a) uniform fibers (low wheel speed), and (b) fibers exhibiting waves (rapid wheel speed).

tip, which cause separation of the fiber from the wheel. When the solidified fiber is airborne (final stage or region 3) it is cooled by radiation and convection since there is no longer contact with the wheel (i.e. no conductive cooling). This lowers the overall cooling rates of the fiber.

The wheel tip is also crucial to melt extraction and its radius determines the dimensions and shape of the extracted fibers, as well as their quality. For a sharp wheel tip, the contact area between the liquid drop and wheel tip decreases. Therefore, the extracted fibers tend to be thinner and more flexible. Fig. 6 shows the tip of a copper wheel in cross-section that has been successfully used to extract ceramic fibers.

The chemical composition of the as-extracted fibers was analyzed by inductively coupled plasma atomic emission spectrometer (ICP-AES) in order to check the compositional homogeneity and establish whether material losses were encountered due to the melting process. Results are shown in Table 2. In general, fibers extracted from rods of E1, Y:Al = 3:5 and E2 compositions retained their stoichiometry. In all cases a slight decrease in the alumina content may be caused by vaporization of Al_2O_3 during melting and extracting of the fibers.

3.2. XRD and DSC results

X-ray diffraction patterns for yttria-alumina fibers are shown in Fig. 7. X-ray patterns suggest that the as-extracted fibers are non-crystalline, but not completely amorphous in the case of E2. Furthermore, they were found to be optically transparent. The above observation demonstrates the good glass-forming properties of the yttria-alumina material under rapid solidification conditions. The cooling rate of the present process was estimated previously to be in the order of 10^5 K s^{-1} for a 10 μm diameter ceramic fiber.[25,26] It is noticeable that the cooling rate depends upon various parameters such as the wheel velocity, thickness of the fibers and adhesion to the wheel tip.

The thermal evolution of glass fibers was followed by means of DTA and XRD identification of the resulting phases. The DTA curves at a heating rate of 20°C/min denote a small endothermic effect that is due to the glass transition and is identified as the T_g temperature. The DTA curve for E1 fibers indicates two independent exothermic peaks at 949 and 1040°C. The DTA trace of composition Y:Al = 3:5 exhibits a sharp peak around 942°C. YAG fibers prepared by other processes such as the sol–gel route and chemical precursor route (yttrium and aluminum nitrates) also showed a similar peak around 900–950°C in the DTA trace.[17,21] Composition E2 exhibited one narrow peak at 939°C (Fig. 8a).

The equilibrium phases encountered after heat treatment were $Y_3Al_5O_{12}$, (YAG) and α-Al_2O_3 (corundum) in the sequence for E1; phase pure $Y_3Al_5O_{12}$ (YAG) for

Table 2
Chemical composition (wt%) of as-extracted fibers analyzed by ICP-AES

Composition	Al_2O_3	Y_2O_3
E1	62.1	37.9
Y:Al = 3:5	42.3	57.7
E2	36.7	63.3

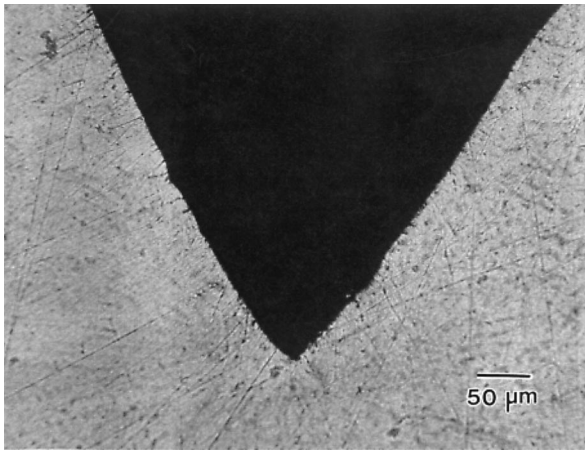

Fig. 6. Wheel tip of a copper wheel used for melt extraction.

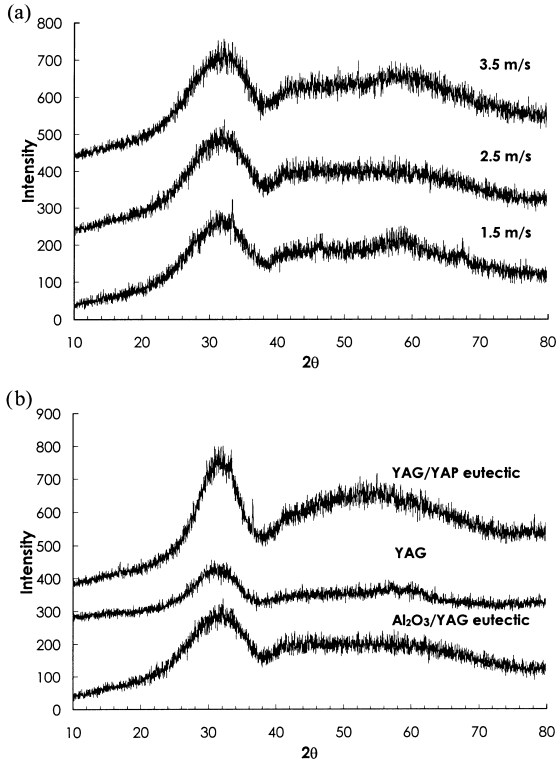

Fig. 7. X-ray diffraction patterns of Y_2O_3–Al_2O_3 fibers: (a) E1 fibers at 1.5, 2.5 and 3.5 m/s extraction velocities, and (b) E1, Y:Al = 3:5 and E2 fibers extracted at 1.5 m/s.

Y:Al = 3:5; and cubic perovskite $YAlO_3$ (YAP) for E2 (Fig. 8b). These phases are in complete agreement with Y_2O_3–Al_2O_3 phase diagram, except for E2 in which was expected to find YAG and YAP after heat treatment. However, the phase development in the E2 composition occurs gradually during heating, forming a sequence of intermediate phases. These can be followed through the X-ray diffraction patterns taken from short fibers heated for 1 hour at various temperatures. The X-ray diffraction pattern for E2 fibers heat-treated at 1500°C for 1 h with a heating rate of 10°C/min (Fig. 8b) indicates the presence of YAG and YAP orthorhombic perovskite as a second phase.

3.3. Tensile testing

Tensile strength tests of glass fibers were performed at room temperature in an Instron tensile machine. The actual diameters, obtained by microscopic examination of the fractured fibers, were used in the calculation of strength values and are presented in Fig. 9.

It is observed from Fig. 9(a) that as the wheel velocity increases the tensile strength decreases because of the discontinuities along the fiber. As wheel velocity increases, the morphology of the ceramic fibers tends to change from uniform circular cross section to those exhibiting waves, which introduce defects and stress raisers into the fibers. Moreover, the tensile strength of the fibers decreases as the alumina content increases. However, it was noticed that with a higher alumina content, the average diameter of the extracted fibers was larger [Fig. 9(b)], and therefore the flaws population and defects size in the fibers could be larger. It is believed that the addition of yttria into the mixture decreases the viscosity of the liquid ceramic facilitating the extraction of a thinner layer. It was previously suggested[24] that in the extraction of liquid ceramics, momentum is transferred much more rapidly than heat, which is the controlling mechanism for fiber extraction. In this mechanism, momentum penetrates into the liquid through viscosity, hence viscosity plays an important role in the system and also in determining the dimensions of the extracted layer. Viscosity, like surface tension, usually decreases as the temperature increases above the melting temperature (liquidus). Therefore, extraction from a molten drop exhibiting a low viscosity drags out a thin layer, which could be rapidly quenched

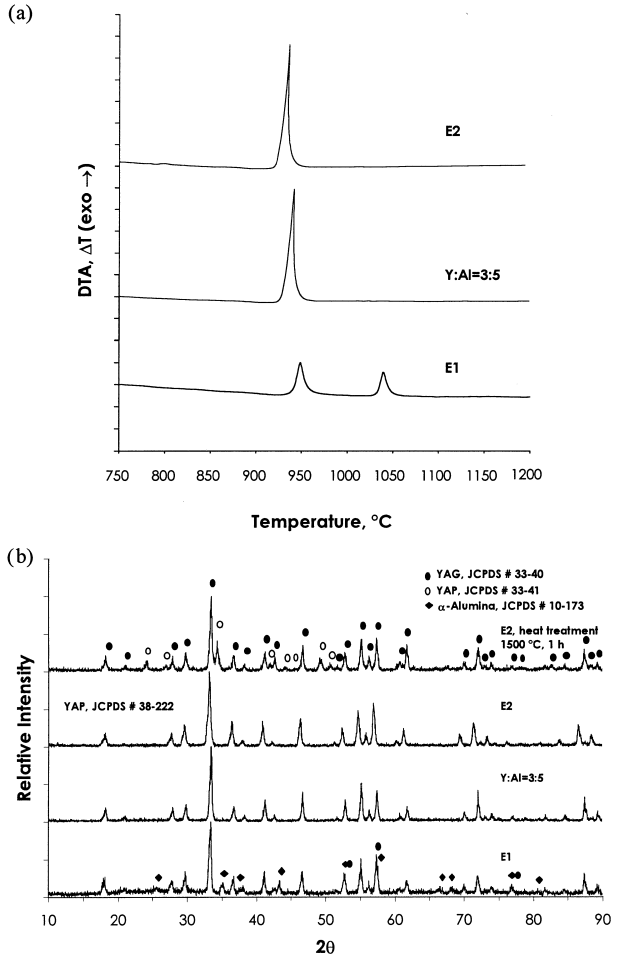

Fig. 8. (a) DTA curve of Y_2O_3–Al_2O_3 glass fibers heated at 20°C/min; and (b) XRD patterns of Y_2O_3–Al_2O_3 glass fiber.

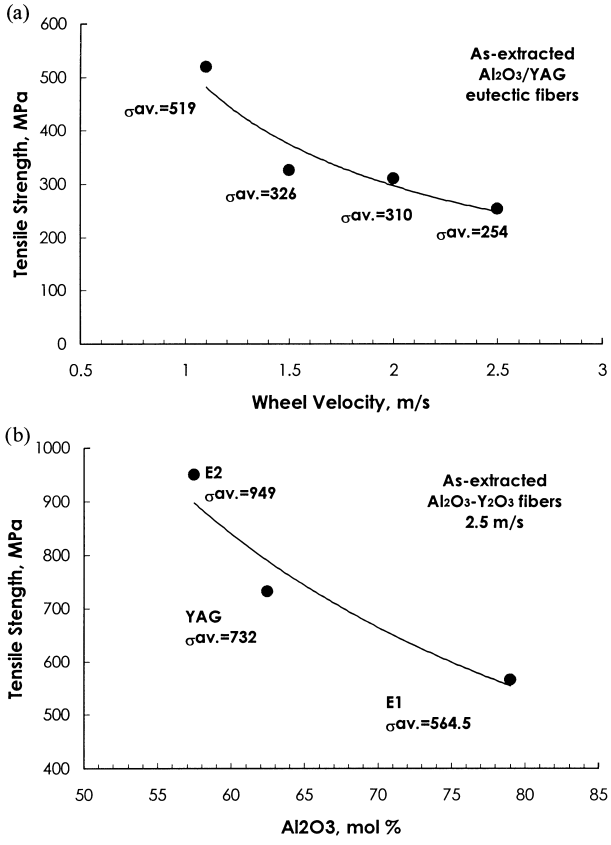

Fig. 9. Tensile strength results for as-produced fibers as a function of: (a) wheel velocity, and (b) Al_2O_3 content.

to form a fiber. However, extraction from a more viscous liquid (e.g. liquid closer to its liquidus) pulls out a thicker layer, which may disintegrate prior to solidification owing to insufficient heat removal by the wheel tip and the larger heat content of that layer.

The scatter in the tensile strengths of the fibers can be attributed to the variation in diameter of the fibers, imperfections and flaws in the surface of the fiber, and may also result from handling damage after processing. Any imperfection on the wheel tip, which is replicated onto the fiber surface, causes deterioration of the tensile properties of the fibers, and introduces flaws and other sources of scatter.

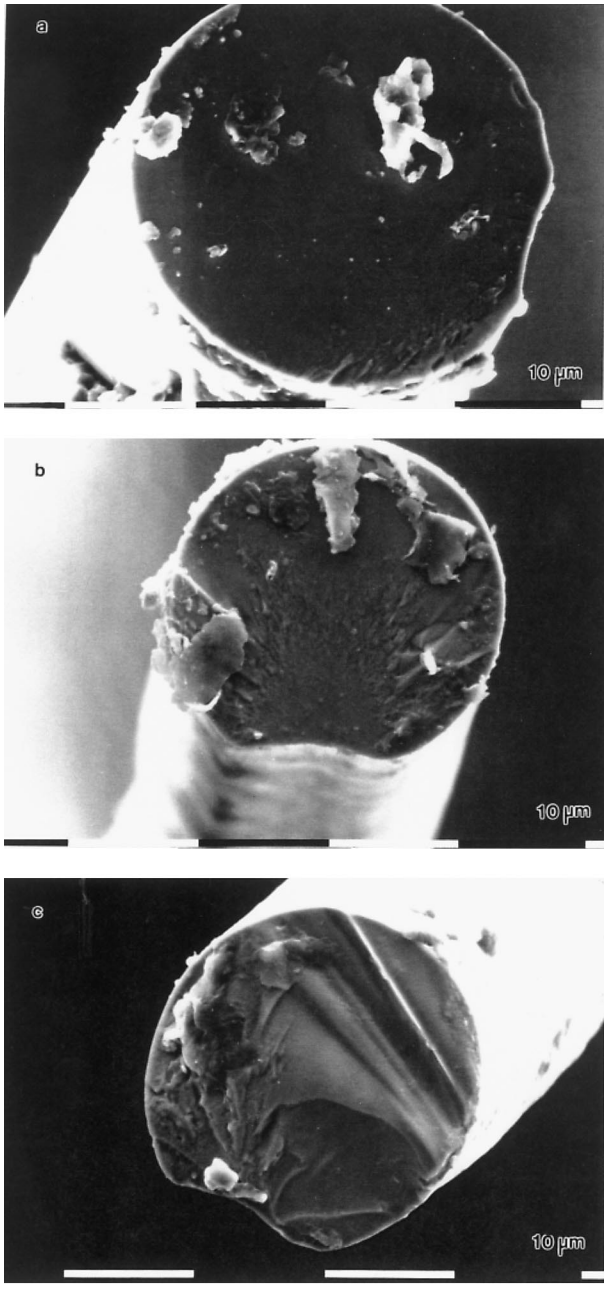

Fig. 10. Fracture surface SEM micrographs after tensile testing at room temperature of as-produced fibers: (a) E1, (b) Y:Al = 3:5, and (c) E2.

Fig. 10 shows the fracture surface after tensile testing of as-extracted fibers at room temperature. It can be seen that the fracture was brittle and always initiated from flaws on the fiber surface caused by the extraction process and related to the wheel track. Flaws in a ceramic material concentrate the stress, fracture occurs when the stress at the flaw reaches a critical value sufficient to initiate and extend a crack.[29]

The modulus of elasticity for amorphous fibers were calculated using the equation $E = \sigma/\varepsilon = (\sigma \cdot L_0)/\Delta L$, where σ is the fracture stress, L_0 is the gauge length (initial length) and ΔL is the deformation. The values of elastic modulus of amorphous yttria–alumina fibers are 140, 129, and 162.5 GPa for E1, Y/Al = 3:5, and E2, respectively, and are lower than the corresponding crystalline materials. Crystalline yttria and alumina have an elastic modulus of 174.4 and 380 GPa, respectively,[29,30] and the rule of mixtures was used to calculate the elastic modulus of E1, Y:Al = 3:5, and E2 crystalline counterparts. The calculated elastic modulus for E1, Y:Al = 3:5, and E2 are 336.8, 302.9 and 292.6 GPa, respectively.

These moderated values of modulus of elasticity are attributed to the amorphous nature of the fibers. The magnitude of the elastic modulus is determined by the strength of the atomic bonds in the material. The stronger the atomic bonding, the greater the stress required to increase the interatomic spacing, and thus the greater the value of the modulus of elasticity. The more open structure, weaker bonding and lower coordination number of an amorphous structure result in moderate to low elastic modulus.[29]

4. Conclusions

1. It was demonstrated that various yttria–alumina compositions could be successfully melt extracted.
2. The fibers morphology is markedly influenced by the wheel velocity. The lower the wheel velocity, the more uniform is the cross section of the fibers.
3. Regardless of the wheel velocity and composition, all extracted fibers were amorphous, which demonstrates the glass-forming properties of the yttria-alumina material.
4. After DTA heat treatment of the amorphous Y_2O_3–Al_2O_3 fibers, the phases encountered were YAG and α-Al_2O_3 for E1, YAG for Y:Al = 3:5 and YAP cubic perovskite for E2. The complete phase development for E2 was achieved after heat treatment at 1500°C for 1 h with the presence of YAG and YAP orthorhombic perovskite.
5. The tensile strength of the as-extracted fibers decreased as the wheel velocity and alumina content

increased due to the increase in fiber diameter and as well as the viscosity.

6. The tensile strength results showed a large scatter that can be attributed to the several sources of defects in the fibers, for instance, cross sectional discontinuities along the fiber and the presence of the wheel track.

Acknowledgements

The authors wish to thank DLR (Deutsche Forschungsanstalt für Luft- und Raumfahrt, Cologne, Germany) for providing access to the facilities for experimental data. We would like also to acknowledge to CONACYT (Consejo Nacional de Ciencia y Tecnologia, Mexico) for granting a scholarship to E.A. Aguilar and NSERC (Natural Sciences and Engineering Research Council of Canada) for partial support of this research.

References

1. Chawla, K. K., *Composites Materials: Science and Engineering*. Springer-Verlag, New York, 1987.
2. Cahn, R. W., Haasen, P. and Kramer, E. J., *Materials Science and Technology, Vol. 13: Structure and Properties of Composites*, ed. Tsu-Wei Chou. VCH, 1991.
3. DiCarlo, J. A., Fibers for structurally reliable metal and ceramics composites. *Journal of Metals*, 1995, June, 44–49.
4. Nair, S. V. and Jakus, K., eds. *High Temperature Mechanical Behavior Of Ceramic Composites*. Butterworth-Heinemann, 1995.
5. Newcomb, S. A. and Tressler, R. E., Slow crack growth in sapphire fibers at 800° to 1500°C. *J. Am. Ceram. Soc.*, 1993, **76**(10), 2505–2512.
6. Ikesue, A., Kinoshita, T., Kamata, K. and Yoshida, K., Fabrication and optical properties of high-performance polycrystalline Nd:YAG ceramics for solid-state lasers. *J. Am. Ceram. Soc.*, 1995, **78**(4), 1033–1040.
7. Keller, K., Mah, T. and Parthasarathy, T. A., Processing and mechanical properties of polycrystalline $Y_3Al_5O_{12}$ (yttrium aluminum garnet). *Ceram. Eng. Sci. Proc.*, 1990, **11**(7–8), 1122–1133.
8. Mah, T., Parthasarathy, T. A. and Matson, L. E., Processing and mechanical properties of $Al_2O_3/Y_3Al_5O_{12}$ (YAG) eutectic composite. *Ceram. Eng. Sci. Proc.*, 1990, **11**(9–10), 1617–1627.
9. Parthasarathy, T. A., Mah, T. and Matson, L. E., Creep behavior of $Al_2O_3/Y_3Al_5O_{12}$ eutectic composite. *Ceram. Eng. Sci. Proc.*, 1990, **11**(9–10), 1628–1638.
10. Parthasarathy, T. A., Mah, T. and Keller, K., High-temperature deformation behavior of polycrystalline yttrium aluminum garnet (YAG). *Ceram. Eng. Sci. Proc*, 1991, **12**(9–10), 1767–1773.
11. Parthasarathy, T. A., Mah, T. and Keller, K., Creep mechanism of polycrystalline yttrium aluminum garnet. *J. Am. Ceram. Soc.*, 1992, **75**(7), 1756–1759.
12. Parthasarathy, T. A., Mah, T. and Matson, L. R., Deformation behavior of an Al_2O_3–$Y_3Al_5O_{12}$ eutectic composite in comparison with sapphire and YAG. *J. Am. Ceram. Soc.*, 1993, **76**(1), 29–32.
13. Mah, T., Parthasarathy, T. A., Petry, M. D. and Matson, L. E., Processing, microstructure, and properties of Al_2O_3–$Y_3Al_5O_{12}$ (YAG) eutectic fibers. *Ceram. Eng. Sci. Proc.*, 1993, **14**(7–8), 622–638.
14. Farmer, S. C., Sayir, A., Dickerson, P. O. and Draper, S. L., Microstructural stability and strength retention in directionally solidified Al_2O_3–YAG eutectic fibers. *Ceram. Eng. Sci. Proc.*, 1995, **16**(5), 969–976.
15. Doleman, P. A. and Butler, E. G., The growth of alumina/YAG eutectic fibers by the laser heated floating zone process. *Key Engineering Materials*, 1997, **127–131**, 193–202.
16. Morscher, G. N., Chen, K. C. and Mazdiyasni, K. S., Creep-resistance of developmental polycrystalline yttrium–aluminum garnet fibers. *Ceram. Eng. Sci. Proc.*, 1994, **15**(4), 181–188.
17. King, B. H., Liu, Y., Laine, R. M. and Halloran, J. W., Fabrication of yttrium aluminate fibers. *Ceram. Eng. Sci. Proc.*, 1993, **14**(7–8), 639–650.
18. King, B. H. and Halloran, J. W., Polycrystalline yttrium aluminum garnet fibers from colloidal sols. *J. Am. Ceram. Soc.*, 1995, **78**(8), 2141–2148.
19. Glaubitt, W., Watzka, W., Scholz, H. and Sporn, D., Sol–gel processing of functional and structural ceramic oxide fibers. *J. Sol–Gel Sci. Technol.*, 1997, **8**, 29–33.
20. Pullar, R. C., Taylor, M. D. and Bhattacharya, A. K., The manufacture of yttrium aluminum garnet (YAG) fibres by blow spinning form a sol–gel precursor. *J. Eur. Ceram. Soc.*, 1998, **18**(12), 1759–1764.
21. Popovich, D., Lombardi, J. and King, B. H., Fabrication and mechanical properties of polymer melt spun yttrium aluminum garnet (YAG) fiber. *Ceram. Eng. Sci. Proc.*, 1997, **18**(3), 65–72.
22. Zhu, D., Jilavi, M. H. and Kriven, W. M., Synthesis and characterization of mullite and YAG fibers grown from deeply undercooled melts. *Ceram. Eng. Sci. Proc.*, 1997, **18**(3), 31–38.
23. Strom-Olsen, J. O. and Rudkowski, P. Z., Apparatus and method for fabrication of metallic fibers having a small cross section. U.S. Patent No. 5027886, 1991.
24. Allahverdi, M., Drew, R. A. L. and Ström-Olsen, J. O., Melt-extracted oxide ceramic fibres — the fundamentals. *J. Mat. Sci.*, 1996, **31**, 1035–1042.
25. Ström-Olsen, J. O., Rudkowska, G., Rudkowski, P., Allahverdi, M. and Drew, R. A. L., Fine metallic and ceramic fibers by melt extraction. *Mat. Sci. Eng.*, 1994, **A179/A180**, 158–162.
26. Ström-Olsen, J., Fine fibres by melt extraction. *Mat. Sci. Eng.*, 1994, **A178**, 239–243.
27. Roth, R. S., *Phase Equilibria Diagrams, Phase Diagrams for Ceramists*, Vol. XI. Compiled at the National Institute of Standards and Technology. The American Ceramic Society, 1995, p. 132, Fig. 4370.
28. Allahverdi, M., Drew, R. A. L., Rudkowka, P., Rudkowski, G. and Strom-Olsen, J. O., Amorphous $CaO{\cdot}Al_2O_3$ fibers by melt extraction. *Mat. Sci. Eng.*, 1996, **A207**, 12–21.
29. Richerson, D. W., *Modern Ceramic Engineering: Properties, Processing, and Use in Design*. Dekker, 1992 (Chapter 5).
30. Watchman, J. B., *Mechanical Properties of Ceramics*. John Wiley & Sons, 1996 (Chapter 3).